American Mineralogist, Volume 91, pages 929–936, 2006

Pseudojohannite from Jáchymov, Musonoï, and La Creusaz: A new member of the zippeite-group

JOËL BRUGGER,[1,2,*] KIA SHEREE WALLWORK,[3,†] NICOLAS MEISSER,[4] ALLAN PRING,[1] PETR ONDRUŠ,[5] AND JIŘÍ ČEJKA[6]

[1]South Australian Museum, North Terrace, Adelaide, South Australia 5000, Australia
[2]School of Earth and Environmental Sciences, University of Adelaide, Adelaide, South Australia 5005, Australia
[3]Bragg Institute, ANSTO, PMB 1, Menai, New South Wales 2234, Australia
[4]Museum of Geology and Institute of Mineralogy and Geochemistry, University, UNIL-BFSH-2, CH 1015 Lausanne, Switzerland
[5]Czech Geological Survey, Geologická 6, CZ–15200 Prague, Czech Republic
[6]National Museum, Václavské nám. 68, CZ–11579 Prague 1, Czech Republic

ABSTRACT

Pseudojohannite is a hydrated copper(II) uranyl sulfate described from Jáchymov, Northern Bohemia, Czech Republic (type locality). Pseudojohannite also occurs at the Musonoï quarry near Kolwezi, Shaba, Congo, and the La Creusaz prospect, Western Swiss Alps. At all three localities, pseudojohannite formed through the interaction of acid sulfate mine drainage waters with uraninite (Jáchymov and La Creusaz) or uranyl silicates (Musonoï). Pseudojohannite forms moss green, non UV-fluorescent aggregates consisting of irregularly shaped crystals measuring up to 25 μm in length and displaying an excellent cleavage parallel to ($\bar{1}$01). d_{meas} is 4.31 g/cm^3, d_{calc} 4.38 g/cm^3, and the refractive indices are n_{min} = 1.725 and n_{max} = 1.740.

A high-resolution synchrotron powder diffraction pattern on the material from Musonoï shows that pseudojohannite is triclinic (*P*1 or *P*$\bar{1}$), with a = 10.027(1) Å, b = 10.822(1) Å, c = 13.396(1) Å, α = 87.97(1)°, β = 109.20(1)°, γ = 90.89(1)°, V = 1371.9(5) Å^3. The location of the uranium and sulfur atoms in the cell was obtained by direct methods using 1807 reflections extracted from the powder diffractogram. Pseudojohannite contains zippeite-type layers oriented parallel to ($\bar{1}$01). The empirical chemical formula calculated for a total of 70 O atoms is $Cu_{6.52}U_{7.85}S_{4.02}O_{70}H_{55.74}$, leading to the simplified chemical formula $Cu_{6.5}[(UO_2)_4O_4(SO_4)_2]_2(OH)_5{\cdot}25H_2O$. The distance of 9.16 Å between the uranyl-sulfate sheets in pseudojohannite shows that neighboring layers do not share O atoms with the same $Cu\Phi_6$ [Φ = (O,OH)] distorted octahedrons, such as in magnesium-zippeite. Rather, it is expected that $Cu\Phi_6$ forms a layer bound to the zippeite-type layers by hydrogen bonding, as in marécottite, or one apex of the $Cu\Phi_6$ polyhedron only is shared with a zippeite-type layer, as in synthetic SZIPPMg. The higher number of cations in the interlayer of pseudojohannite (Cu:S = 1.6:1) compared to marécottite (3:4) and SZIPPMg (1:1) indicates that pseudojohannite has a unique interlayer topology.

Ab-initio powder structure solution techniques can be used to obtain important structural information on complex micro-crystalline minerals such as those found in the weathering environment. Pseudojohannite represents a new member of the zippeite group of minerals, and further illustrates the structural complexity of zippeite-group minerals containing divalent cations, which have diverse arrangements in the interlayer. Peudojohannite and other divalent zippeites are common, easily overlooked minerals in acid drainage environments around uranium deposits and wastes.

Keywords: New mineral, pseudojohannite, uranyl sulfate, XRD data, IR spectroscopy, Jáchymov, La Creusaz, Musonoï

INTRODUCTION

Pseudojohannite (IMA-2000-019) was described as a new mineral from Jáchymov (St. Joachimsthal), Northern Bohemia, Czech Republic (Ondruš et al. 1997, 2003), with chemical formula $Cu_5(UO_2)_6(SO_4)_3(OH)_{16}{\cdot}14H_2O$ and a triclinic unit cell with a = 13.754(2) Å, b = 9.866(1) Å, c = 8.595(2) Å, α = 103.84(2)°, β = 90.12(2)°, γ = 106.75(2)°, V = 1081.3 (4) Å^3. The mineral name acknowledges the chemical and paragenetical relationship with johannite $Cu(UO_2)_2(SO_4)_2(OH)_2{\cdot}8H_2O$ (Mereiter 1982).

This paper describes two new occurrences of this rare uranyl sulfate mineral at Musonoï, Shaba, Congo, and La Creusaz, Western Swiss Alps. Based on analysis of the synchrotron powder diffraction patterns obtained on pseudojohannite from Musonoï, we redefine the unit cell, and consequently the chemical formula of pseudojohannite, and demonstrate that pseudojohannite belongs to the zippeite-group of minerals. Because the mineralogical data on pseudojohannite are only briefly described in two separate publications (Ondruš et al. 1997, 2003), we also present a complete description of the holotype material.

* E-mail: joel.brugger@adelaide.edu.au
† Current Address: Australian Synchrotron, 800 Blackburn Road, Clayton, Victoria 3168, Australia.

0003-004X/06/0506–929$05.00/DOI: 10.2138/am.2006.1885

The holotype of pseudojohannite from Jáchymov has been split and part is deposited in the mineralogical collection of the National Museum Prague (Czech Republic) under number P1p 1/2000 and the other part at the Geological Museum of Lausanne (Switzerland) under sample number MGL 79290. Pseudojohannite samples from Musonoï and La Creusaz are deposited at the Geological Museum of Lausanne (Switzerland) under sample numbers MGL 54110 and 58324, respectively.

Occurrences

To date, only one sample from the Rovnost (Werner) shaft at Jáchymov (Northern Bohemia, Czech Republic) is known to contain pseudojohannite. In this sample, pseudojohannite grows directly on strongly weathered uraninite containing pyrite, tennantite, and chalcopyrite (Ondruš et al. 1997, 2003) and is associated with johannite, uranopilite, and gypsum. Pseudojohannite forms earthy moss green, brittle aggregates up to 5 mm or coatings with an uneven surface, which are composed of very fine crystals with sizes between 1 and 10 μm. Pseudojohannite shows no fluorescence under UV light. The measured density of pseudojohannite from Jáchymov is 4.31 g/cm^3, d_{calc}= 4.38 g/cm^3 (using the pseudo-monoclinic zippeite cell), and the refractive indices are: n_{min} = 1.725 and n_{max} = 1.740 (Ondruš et al. 1997, 2003).

At the Musonoï quarry near Kolwezi (Shaba, Congo), light green pseudojohannite appears in association with yellow uranopilite and orange-yellow metaschoepite on a saccharoidal quartz matrix containing many crosscutting veins of kasolite, α-uranophane, and cuprosklodowskite (sample MGL 54110). Other associated mineral species are relic Se-bearing digenite, malachite, and a pale blue brochantite. The excellent cleavage of pseudojohannite is visible on SEM photographs (Fig. 1). The crystals measure up to 25 μm in length, and are flattened along the cleavage plane. They coat several cm^2 of tiny open veins. Three specimens of this unique mineral association were bought in 2002 by the Geological Museum of Lausanne from the Swiss mineral dealer François Pahud. These samples were collected by local miners in 1998–2002.

At the La Creusaz U-deposit near Les Marécottes village (canton Valais, Western Alps, Switzerland), pseudojohannite is directly associated with gypsum, johannite, ktenasite, marécottite (type locality; Brugger et al. 2003), and uranopilite in a broader paragenesis that also contains Al-bearing coconinoite, jáchymovite, jarosite, rabejacite, schröckingerite, zippeite *s.s.*, magnesium-zippeite, and zeunerite (Meisser 2003; Meisser et al. 2002). These minerals encrust blocks of primary ore consisting mainly of uraninite and quartz. Pseudojohannite forms moss green earthy aggregates up to 3 mm in size; these aggregates are constituted by poorly shaped crystals ~10 μm in length.

La Creusaz was explored by drilling, surface scratching, and galleries between 1973–1981 (Meisser 2003; Meisser et al. 2002). Since the end of the underground exploration in 1981, outcropping veins and stockpiled U-ore have been exposed to acid mine drainage water and atmospheric oxygen in the abandoned galleries. The oxidation of the sulfides (mainly pyrite and chalcopyrite) resulted in the production of acid (pH ≥ 3.1), sulfate-rich waters. These waters reacted with uraninite, chamosite, calcite, and siderite to form a rich assemblage of secondary uranyl minerals, including several sulfates. Pseudojohannite samples were collected among the ore stockpiled in the exploration gallery at La Creusaz, which remained undisturbed since 1981.

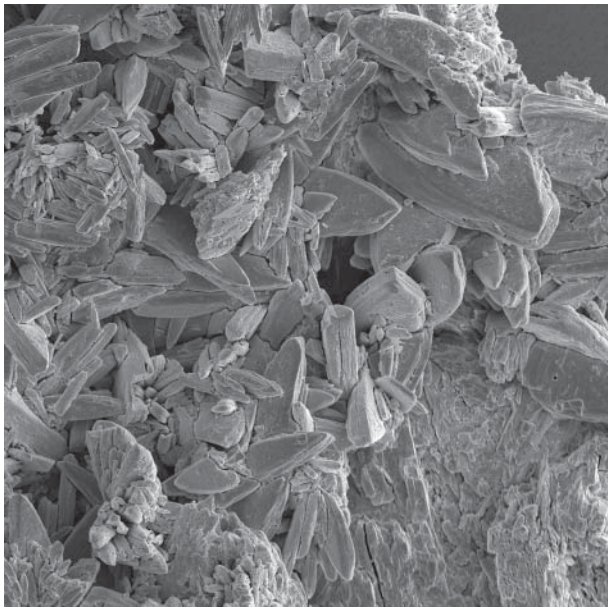

Figure 1. SEM microphotograph of pseudojohannite crystals from Musonoï (sample MGL 54110). Image width: 50 μm.

Hence, at La Creusaz, pseudojohannite forms through the interaction of acid sulfate water resulting from the oxidation of pyrite and chalcopyrite, with uraninite. A similar genesis is probable at Jáchymov. At Musonoï, the acid drainage waters probably result mainly from the oxidation of Se-digenite, and pseudojohannite subsequently forms through the reaction with oxidized U-bearing minerals such as kasolite, α-uranophane, and cuprosklodowskite.

The identification of the material is based on qualitative chemical analyses showing that the three minerals consist only of U, O, S, and Cu, and on the similarity in the X-ray powder diffraction patterns (Table 1).

X-ray powder diffraction (Musonoï)

Experimental methods

An almost pure sample was loaded into a 0.3 mm diameter silica glass capillary without further crushing. The diffraction pattern was recorded using synchrotron radiation in the high-resolution powder diffractometer at the Australian National Beamline Facility (ANBF) BL-20B at the Photon Factory (KEK), Tsukuba, Japan, (Garrett et al. 1995). Partial diffraction rings were collected on three adjacent image plates, located 573 mm from the axially spinning sample. Data were collected at a wavelength of 1.4985(2) Å, calibrated by using an alumina reference standard (NBS 674). The data were extracted from the image plates and processed using the program Python PDA (Hester et al. 1999). The angular range of the data was 6.00–43.00°, 43.23–83.10°, 83.50–120.00°, in steps of 0.010° of 2θ. Even though the image plates are butted together a small gap (~0.3°) occurs. For structure analysis and refinement the RIETICA (Hunter 1998) and SIRPOW.92 (Altomare et al. 1994) packages were used.

Unit-cell determination

Attempts to index the pattern using the cell data of Ondruš et al. (2003) were unsuccessful and a new triclinic cell was obtained using the program ITO (Visser 1969). This cell, where a = 8.880

TABLE 1. X-ray powder diffraction pattern of pseudojohannite

				Musonoï[1]			Jáchymov[2]		
No.	*h*	*k*	*l*	d_{calc}	I_{calc}	d_{obs} (Å)	I_{obs}	d_{obs} (Å)	I_{obs}
1.						20.487	1		
2.	0	0	1	12.6	<0.1			13.2	7
3.	1	0	$\bar{1}$	9.16	100	9.18	100	9.13	100
4.	0	1	1	8.35	12	8.37	6	8.33	7
5.						8.188	2		
6.						7.921	2		
7.	1	1	0	7.11	8	7.121	22	7.09	26
8.	1	0	1	6.609	0.3	6.625	0.9		
9.	$\underline{0}$	0	2	6.322	0.5	6.332	0.8	6.308	1
10.	$\bar{1}$	0	2	6.300	<0.1	6.26	0.1		
11.*						6.087	0.2		
12.	$\underline{0}$	1	2	5.536	<0.1	5.535	13	5.511	22
	$\bar{1}$	1	2	5.528	5				
13.	0	2	$\underline{0}$	5.408	<0.1	5.43	0.4		
14.	1	1	$\bar{2}$	5.364	0.4	5.369	1.2	5.351	3
15.*						4.843	0.4		
16.*						4.820	0.4		
17.*						4.795	0.1		
18.	$\underline{2}$	0	0	4.735	2	4.739	2	4.721	6
19.	$\bar{1}$	2	$\underline{1}$	4.713	0.2	4.717	0.2		
20.	$\underline{1}$	2	$\bar{1}$	4.602	0.2	4.615	0.5		
21.	$\bar{2}$	0	$\underline{2}$	4.580	20	4.584	53.2	4.566	80
22.	2	1	$\bar{1}$	4.514	2	4.518	1.2		
23.	1	0	3	4.429	2	4.433	2.9	4.419	8
24.*						4.293	0.4		
25.	1	1	2	4.270	<0.1	4.273	0.7		
26.	1	$\underline{2}$	1	4.214	3	4.215	5.9	4.200	10
	1	$\bar{1}$	2	4.205	3				
27.	0	$\underline{2}$	2	4.176	3	4.179	4.2	4.166	8
28.	$\underline{1}$	$\bar{2}$	1	4.157	3	4.158	0.9		
29.	$\bar{1}$	1	3	4.151	<0.1	4.147	2.2		
30.*						4.090	0.9		
31.	0	$\bar{2}$	2	4.046	3	4.048	7.7	4.036	8
32.	0	1	3	3.970	0.1	3.973	1.0	3.963	2
33.*						3.956	0.9		
34.	0	$\underline{1}$	$\bar{3}$	3.885	2	3.887	4.4	3.874	6
36.	2	$\bar{1}$	1	3.761	2	3.763	6.5	3.752	7
37.*						3.739	1.1		
38.	$\bar{2}$	1	3	3.653	2	3.654	1.2	3.645	4
39.	0	3	0	3.605	<0.1	3.601	0.1		
40.	2	$\bar{2}$	0	3.569	2	3.571	4.7	3.560	9
41.	$\underline{2}$	2	0	3.555	2	3.556	2.0		
42.	$\bar{2}$	2	2	3.543	0.4	3.544	0.5		
43.*						3.527	<1		
44.*						3.511	<1		
45.	0	3	1	3.497	<0.1	3.497	0.6		
46.	$\bar{1}$	$\underline{2}$	3	3.488	2	3.489	3.2	3.480	6
47.	1	$\bar{2}$	2	3.470	<0.1	3.474	2.2		
48.	1	0	$\underline{3}$	3.452	12	3.454	18.0	3.443	17
	2	$\underline{2}$	$\bar{2}$	3.449	0.4				
49.	0	$\underline{3}$	1	3.438	12	3.439	12.6		
50.	1	3	$\underline{0}$	3.374	11	3.375	18.9	3.367	15
51.	1	2	3	3.368	2	3.367	1.3		
	1	3	$\underline{0}$	3.365	0.2				
52.	3	0	$\bar{1}$	3.330	2	3.332	3.1	3.321	11
53.	$\underline{2}$	0	2	3.304	10	3.306	16.4	3.298	13
54.	$\bar{1}$	1	4	3.230	0.3	3.208	0.9		
55.	$\underline{0}$	0	4	3.161	9	3.162	15.8	3.154	15
56.	$\bar{2}$	0	4	3.150	2	3.151	2.8		
57.	3	1	$\bar{2}$	3.128	0.9	3.129	1.5	3.122	8
58.	1	3	$\bar{2}$	3.083	8	3.084	16.7		
59.	3	0	$\bar{3}$	3.053	6	3.054	9.1	3.046	26
60.	3	1	$\underline{0}$	3.027	0.2	3.028	0.7		
62.	$\underline{2}$	1	4	2.997	<0.1	2.994	1.0		
63.	$\bar{2}$	3	1	2.950	7	2.950	9.6	2.945	10
64.	1	2	$\underline{3}$	2.943	<0.1	2.930	0.6		
65.	3	1	3	2.918	<0.1	2.912	0.3		
66.	1	3	2	2.869	7	2.869	18.8	2.862	20
67.	$\bar{3}$	2	1	2.852	0.9	2.851	7.7	2.845	10
	3	0	$\underline{1}$	2.850	6				
68.	3	2	$\bar{1}$	2.820	1	2.820	1.1		
69.	0	3	3	2.784	7	2.784	11.9		
70.	$\underline{0}$	2	4	2.768	0.1	2.767	0.7		
	$\bar{2}$	2	4	2.764	1				
71.	0	4	0	2.704	1	2.704	2.0		
72.	2	3	$\underline{1}$	2.693	6	2.694	6.7	2.687	13
73.	2	2	$\underline{4}$	2.682	1	2.682	2.7		
74.	$\underline{1}$	0	–5	2.672	5	2.673	8.7	2.667	13
75.	3	1	4	2.663	0.7	2.663	3.8	2.66	13
	2	1	3	2.662	0.8				
76.	1	$\bar{1}$	$\underline{4}$	2.640	<0.1	2.636	0.3		
77.	3	2	$\underline{3}$	2.628	0.5	2.629	0.9	2.622	5
78.	$\underline{3}$	1	4	2.624	0.3	2.624	0.7		
79.	$\bar{1}$	4	$\underline{1}$	2.613	0.8	2.613	0.7		
80.	2	3	$\underline{3}$	2.585	4	2.585	2.1	2.580	4
81.	$\underline{1}$	4	$\bar{1}$	2.574	0.6	2.574	0.5		
82.	$\bar{2}$	1	$\underline{5}$	2.564	0.4	2.564	0.8	2.560	2
83.	2	$\underline{1}$	5	2.525	0.2	2.523	1.4		
84.	3	$\bar{2}$	1	2.518	0.1	2.517	0.3	2.517	3
85.	$\underline{4}$	0	$\bar{2}$	2.504	2	2.504	2.1		
86.	$\bar{1}$	3	4	2.497	5	2.497	5.7	2.495	12
87.	$\underline{0}$	1	5	2.480	0.8	2.480	0.3		
88.	$\underline{3}$	$\underline{3}$	2	2.455	4	2.455	3.4	2.4518	5
89.	0	$\bar{1}$	5	2.445	0.1	2.443	0.1		
	3	$\bar{1}$	2	2.443	0.1				
90.	$\bar{1}$	2	5	2.429	0.2	2.429	0.6		
91.	4	1	$\underline{1}$	2.422	0.6	2.422	1.5	2.4183	4
92.	3	3	$\underline{2}$	2.405	1	2.405	1.3		
93.	$\underline{3}$	0	5	2.394	2	2.395	2.1	2.3990	5
94.	4	1	3	2.386	0.5	2.386	0.7	2.3905	8
95.	3	3	0	2.370	4	2.370	7.8	2.3659	13
	$\underline{4}$	0	0	2.367	3				
96.	$\bar{3}$	3	3	2.361	0.1	2.363	1.1		
97.	$\bar{2}$	$\underline{4}$	2	2.357	0.5	2.357	0.5		
98.	$\underline{2}$	4	0	2.352	0.1	2.352	0.4	2.3408	5
99.	$\bar{1}$	4	$\underline{3}$	2.345	0.1	2.344	2.6		
100.	$\underline{2}$	4	$\bar{2}$	2.301	0.4	2.301	0.3		
101.	$\underline{4}$	0	4	2.290	2	2.290	4.7	2.2857	14
102.	4	2	$\underline{2}$	2.287	0.5	2.286	0.5		
103.	1	4	$\underline{3}$	2.272	0.1	2.272	1.0		
104.	$\underline{4}$	2	$\bar{2}$	2.257	0.6	2.257	0.3	2.2537	2
105.	$\bar{2}$	0	6	2.214	3	2.215	2.8	2.2112	6
106.	–3	3	4	2.208	1	2.208	0.8		
107.	3	0	3	2.203	0.2	2.203	1.3		
108.	$\underline{2}$	3	3	2.198	<0.1	2.198	0.2		
109.	$\bar{1}$	1	6	2.187	0.5	2.187	1.0	2.1836	2
110.	$\bar{1}$	3	$\underline{5}$	2.183	<0.1	2.183	<0.1		
111.	3	$\underline{2}$	5	2.163	0.5	2.162	0.3		
112.	2	$\underline{3}$	3	2.159	3	2.159	8.9		
113.	1	3	$\underline{4}$	2.154	6	2.154	11	2.151	12
114.	3	3	$\underline{4}$	2.142	2	2.143	5.2	2.1387	8
	0	5	1	2.143	0.7				
115.	$\underline{2}$	2	4	2.135	0.7	2.135	2.0		
116.	$\underline{4}$	2	4	2.130	0.3	2.130	0.7		
117.	$\underline{3}$	4	1	2.112	0.2	2.112	0.4		
118.	3	4	2	2.110	0.6	2.110	1.9		
119.	1	$\underline{5}$	0	2.107	0.8	2.107	6.5	2.104	8
120.	1	4	3	2.103	0.4	2.103	4.7		
	2	$\bar{2}$	4	2.102	0.6				
121.		3 lines ≤ 0.5				2.088	2.9	2.0845	6
122.	$\underline{2}$	3	–5	2.083	0.8	2.082	1.4		
	4	$\underline{1}$	5	2.081	0.3				
123.	$\underline{2}$	4	2	2.078	0.4	2.078	0.6		
124.	3	1	6	2.075	0.4	2.075	2.7	2.073	4
125.	1	$\bar{2}$	5	2.069	0.6	2.068	3.9		

Notes: (1) Synchrotron radiation, λ = 1.4985(2) Å; (2) Diffractometer Phillips X'Pert System, Cu*Kα* -Ni- filtered radiation, 40 kV, 40 mA. Data from Ondruš et al. (1997) on holotype. Unindexed line in the Musonoï pattern are starred (*); their intensities are ≤1.1%.

Å, b = 10.025 Å, c = 8.686 Å, α = 109.467°, β = 103.994°, and γ = 72.115°, V = 684.7 Å^3, was transformed into a pseudo-monoclinic cell and the cell parameters were refined by fitting the whole data set: a = 10.027(1) Å, b = 10.822(1) Å, c = 13.396(1) Å, α = 87.97(1)°, β = 109.20(1)°, γ = 90.89(1)°, V = 1371.9(5) Å^3. A cell of higher metric symmetry could not be found by cell reduction (Le Page and Flack 1995). The pseudo-monoclinic cell, with a volume about twice that of the reduced cell, was preferred for easy comparison with zippeite-type minerals (see below). The powder data on pseudojohannite from different localities were indexed using this pseudo-monoclinic cell (Table 1). This cell allows all the major lines on the powder diffractogram of Musonoï to be indexed; a few low intensity (≤1.1%) lines are unexplained, and are probably related to impurities: for example, the line at 4.293/0.4 may be gypsum (100%). The original unit cell given by Ondruš et al. (2003) for pseudojohannite is listed in Table 2; this cell does not account for all the significant lines observed in the synchrotron powder diffraction pattern for the Musonoï specimen. The new pseudo-monoclinic cell accounts for all lines in the holotype specimen from Jáchymov. There is no relationship between the unit cell of Ondruš et al. (2003) and the new pseudo-monoclinic cell found in this study, and the former probably represents an artifact of the quality of the data that could be obtained on the holotype.

Structure model and topology

Intensity data were extracted from the powder pattern in the form of F^2_{obs} values using the Le Bail profile fit within RIETICA. The cell parameters, zero error, scale factor, and peak profile parameters for each of the three histograms were refined. A pseudo-Voigt function was used to model the profile shape. The coefficients were refined simultaneously but constrained to be equal for all histograms. Space group $P1$ was chosen for the reflection extraction. This data extraction afforded 4402 reflections, the first 1807 of which were subsequently input into the direct methods program SIRPOW.92 in the form: hkl, FWHM, F^2_{obs}. Of the atomic coordinates given in the direct methods program output, the first eight atoms were found to be U atoms, and the next three atoms were assigned as S atoms. Due to the symmetry observed in the coordinates of the U and S atoms, these atoms were placed at the positions defined by a body-centered cell. Consequently, the space group $I1$ was assigned; the resulting final atomic coordinates are given in Table 3. Using this procedure, the missing, 4th S position that could not be found in the $P1$ refinement was located. The residuals were similar for refinements in $P1$ (9.90%) and $I1$ (9.78%). Note that the body centering ($I1$) relates only to the U and S atomic positions; the mineral itself is triclinic with space group $P1$ or $P\bar{1}$. Although the "heavy" copper atoms were expected to be observed in the direct method solution, they could not be conclusively assigned, despite numerous empirical attempts. Fourier difference maps also failed to reveal the location of the copper atoms.

The topology of the U and S atoms in the structural model presented herein is such that they occur in layers oriented parallel to ($\bar{1}$01); the distance between each layer is 9.16 Å. Within the layers, the U atoms form infinite double chains extending along [$\bar{1}$ 1 $\bar{1}$], separated by a single row of sulfur atoms (Fig. 2). This topology corresponds to the zippeite-type layer (Fig. 2). The case for the zippeite-type structure is also supported by the U:S ratio of 2:1 (Table 4), as in other zippeite structures (Brugger et al. 2003; Burns et al. 2003). IR spectroscopy further supports this conclusion (see below).

Infrared spectroscopy

The IR spectrum of pseudojohannite was recorded using the KBr technique on the type material from Jáchymov (Fig. 3; Table 5). A strong band at 874 cm^{-1} is assigned to the antisymmetric stretching vibration ν_3 $(UO_2)^{2+}$. The wavenumber of this vibration is lower than the wavenumbers observed in the IR spectra of johannite (911 cm^{-1} with a shoulder at 936 cm^{-1}; Čejka et al. 1988), jáchymovite (902–904 cm^{-1}; Čejka et al. 1996), uranopilite (895–900 and 929–931 cm^{-1}; Čejka et al. 1996), rabejacite (901–906 cm^{-1}; Sejkora et al. 2000), and of one of two zippeite groups (~910 cm^{-1}; Čejka 1999). However, the wavenumber of the ν_3 $(UO_2)^{2+}$ of pseudojohannite is comparable with that of the second zippeite group (870 to 883 cm^{-1}; Čejka 1999), which includes zippeite sensu stricto, NH_4^+-zippeite, Co-zippeite, and Zn-zippeite. The close relationship between pseudojohannite and the zippeite-group is further emphasized by the similarity of the IR spectra of pseudojohannite and zippeite (Fig. 3).

The symmetric stretching vibration ν_1 $(UO_2)^{2+}$ may be observed at 831 cm^{-1}; however, there may be a coincidence with the δ U-OH bending vibration. The uranyl bond lengths calculated with the available empirical relations are:

Table 2. Comparison of the chemical formulas and unit-cells parameters of pseudojohannite, marécottite, and magnesium-zippeite

Details	Locality	S. G.	a (Å)	b (Å)	c (Å)	α (°)	β (°)	γ (°)	V (Å^3)
Pseudojohannite, $Cu_{6.5}[(UO_2)_4O_4(SO_4)_2]_2(OH)_5{\cdot}25H_2O$									
Diffractometer (Cu$K\alpha$), cell based on 20 lines.	Jáchymov, Czech Republic	$P1$ or $P\bar{1}$	10.0277	10.8175	13.3955	88.005	109.211	90.864	1362.4(8)
Synchrotron, λ = 1.4985(2) Å, 4402 lines used in refinement.	Musonoï, Congo	$P1$ or $P\bar{1}$	10.027(1)	10.822(1)	13.396(1)	87.97(1)	109.20(1)	90.89(1)	1371.9(5)
Gandolfi Camera (Cu$K\alpha$), cell based on 11 lines.*	La Creusaz, Switzerland		10.03(4)	10.86(3)	13.42(7)	88.0(2)	109.2(4)	91.1(2)	1380(6)
Ondruš et al. 1997.†	Jáchymov, Czech Republic		8.595(2)	9.866(1)	13.754(2)	106.75(2)	90.12(2)	103.84(2)	1081.2
Marécottite $Mg_3(H_2O)_{18}[(UO_2)_4O_3(OH)(SO_4)_2]_2(H_2O)_{10}$									
	La Creusaz, Switzerland	$P\bar{1}$	10.815(4)	11.249(4)	13.851(6)	66.224(7)	72.412(7)	69.95(2)	1422.1(9)
Magnesium-zippeite $Mg(H_2O)_{3.5}(UO_2)_2(SO_4)O_2$									
	Synthetic (structure on Zn-isomorph)	C 2/m	8.654(3)	14.182(6)	17.714(7)		103.92		

*Unit cells refined using the program UnitCell (Holland and Redfern 1997), based on lines clearly indexed from the proposed structural model (Table 3).
† a and c inverted.

TABLE 3. Atomic coordinates for U and S atoms in the pseudojohannite structure, in space group *I*1

Atom	*x*	*y*	*Z*
U1	0.050(6)	0.589(5)	0.747(5)
U2	0.352(5)	0.336(5)	0.978(4)
U3	0.064(5)	0.924(5)	0.746(4)
U4	0.348(6)	0.677(5)	0.977(5)
S1	0.540	0.740	0.240
S2	0.820	0.500	0.500

Note: The coordinates in *P*1 can be obtained by adding positions with (+1/2, +1/2, +1/2).

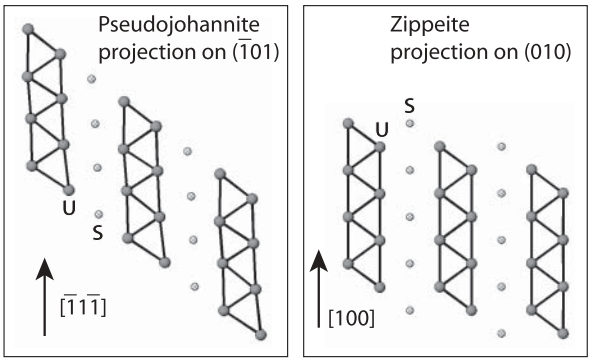

FIGURE 2. Uranyl-sulfate layers in pseudojohannite compared with the layers in zippeite (Burns et al. 2003).

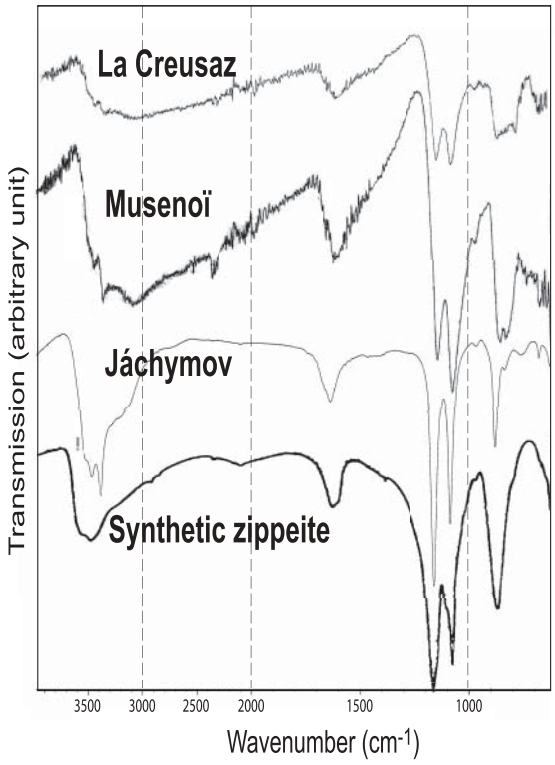

FIGURE 3. Infrared absorption spectrum of pseudojohannite from Jáchymov, Musonoï, and La Creusaz measured with a diamond anvil cell (DAC) compared with the spectra of pseudojohannite from Jáchymov and of synthetic zippeite (Čejka 1999) measured using KBr pellets. See Table 5 for line positions, tentative line assignment and analytical details for the Jáchymov and Musonoï samples.

TABLE 4. Chemical analyses of holotype pseudojohannite from Jáchymov

Constituent	Wt%	Standard deviation	Probe Standard
CuO	14.4	0.49	lammerite
UO_3	62.4	0.77	metallic U
SO_3	8.9	0.15	barite
H_2O	13.95	one TG analysis (Table 7)	
Total	99.65		

Notes: Average of 15 electron microprobe analyses; empirical formula assuming marécottite-type uranyl-sulfate layers, and 70 O atoms pfu: $Cu_{6.52}U_{7.85}S_{4.02}O_{70}H_{55.74}$; simplified empirical fomula: $Cu_{6.5}[(UO_2)_4O_4(SO_4)_2]_2(OH)_5{\cdot}25H_2O$.

TABLE 5. Infrared spectrum of pseudojohannite from Jáchymov (KBr disk) and Musonoï (Diamond cell)

Jáchymov*		Musonoï†		
(cm^{-1})	Intensity	(cm^{-1})	Intensity	Tentative assignment
3520	m,sh	~3496	m, sh	ν OH stretching vibrations of
3453	s	3446	s	hydrogen-bonded water
3375	S	3364	s	molecules and hydroxyl ions
3310	m, sh, b			
3200	m, sh, b	3092	s, b	
1665	m, sh	1654	m, sh	δ H_2O bending vibrations
1627	m	1618	m	of water molecules
1457	vw			δ U-OH bending vibrations
1390	vw			and/or overtones and/or combination bands
1151	vs	1142	vs	$\nu_3 (SO_4)^{2-}$ antisymmetric
1077	vs	1071	vs	stretching vibrations
975	w	1000	s	$\nu_1 (SO_4)^{2-}$ symmetric
		926	w	stretching vibration
874	s	852 to 820	s, b	$\nu_3 (UO_2)^{2+}$ antisymmetric stretching vibration
831	w			$\nu_1 (UO_2)^{2+}$ symmetric stretching vibration or δ U-OH bending vibration
765	w,b			L H_2O libration mode or δ U-OH bending vibration
674	w			$\nu_4 (SO_4)^{2-}$ bending vibrations
625	w			
583	m			
497	w-m			$\nu_2 (SO_4)^{2-}$ bending vibrations
475	w-m			

Notes: Intensity scale: vs = very strong, s = strong, m = medium, w = weak, vw = very weak, character of absorption maxima: sh = shoulder, b = broad.
* Nicolet 740 spectrophotometer; KBr tablets (range 400–4000 cm^{-1}).
† Diamond anvil cell GRAESEBY SPECAC coupled with a Perkin-Elmer PARAGON 1000 FT-IR spectrometer on ground material (range 650–4000 cm^{-1}).

1.804 Å using ($R = 91.41\ \nu_{3,874\ cm-1}^{-2/3} + 0.804$ Å; Barlett and Cooney 1989)
1.796 Å using ($R = 68.2\ \nu_{3,874\ cm-1}^{-2/3} + 1.05$ Å; Glebov 1989)
1.780 Å using ($R = 106.5\ \nu_{1,831\ cm-1}^{-2/3} + 0.575$ Å; Barlett and Cooney 1989)

All these lengths correspond to U-O bond lengths in various other uranyl sulfates and in general agree with uranyl bond distances found in uranyl minerals with U^{6+} in pentagonal bipyramidal coordination (Burns 1999).

The symmetric stretching vibration $\nu_1 (SO_4)^{2-}$ appears as a weak band at 975 cm^{-1}, the doubly degenerate $\nu_2 (SO_4)^{2-}$ bending vibration bands are observed at 497 and 475 cm^{-1}, the triply degenerate $\nu_3 (SO_4)^{2-}$ antisymmetric stretching vibration at 1151 and 1077 cm^{-1}, and the triply degenerate $\nu_4 (SO_4)^{2-}$ bending vibra-

tion bands at 674, 625, and 583 cm^{-1}. This indicates a lowering of the Td symmetry of the $(SO_4)^{2-}$ tetrahedron to C_{2v} or lower. Note that a coincidence of the ν_4 $(SO_4)^{2-}$, H_2O libration modes, and δ U-OH is possible.

The ν OH stretching vibrations of water molecules and hydroxyl ions are observed in the range 3520–3200 cm^{-1}. A band at 1627 cm^{-1} with a shoulder at 1665 cm^{-1} may be attributed to the δ H_2O bending vibrations and shows that at least two types of structurally nonequivalent water molecules are present in the crystal structure of pseudojohannite. Very weak and weak bands at 1457 and 1390 cm^{-1} may be assigned to the δ U-OH bending vibrations and/or overtones and/or combination bands. A weak broad band at 765 cm^{-1} may be connected with the δ U-OH vibration or a H_2O libration mode. Wavenumbers of the ν OH and δ H_2O vibrations indicate that hydrogen bonds of different strengths are involved in the crystal structure of pseudojohannite and a hydrogen-bonding network is established with lengths of the hydrogen bonds approximately 2.70, 2.75, 2.77, 2.85, and 2.95 Å (Libowitzky 1999).

The IR spectra of pseudojohannite from La Creusaz, Musonoï, and part of the holotype from Jáchymov were recorded using a diamond anvil cell (Fig. 3; Table 5). Overall, the spectra are similar to each other, and they closely match the IR spectrum recorded on the Jáchymov material in a KBr tablet. A significant difference, however, appears in the region of stretching vibrations ν_1 and ν_3 of the uranyl ion. The pseudojohannite from La Creusaz and Musonoï exhibits only one broad band in the region 852 to 820 cm^{-1}, while the pseudojohannite from Jáchymov displays well-resolved ν_1 and ν_3 bands. Moreover, the position at which the ν_3 $(UO_2)^{2+}$ band is expected is shifted from 874 cm^{-1} at Jáchymov to 852 cm^{-1} at Musonoï. This difference may indicate slight differences in the hydrogen-bonding network and thus also in the way the interlayer is bound to the zippeite-layers in the pseudojohannite from Jáchymov and La Creusaz/Musonoï. The assignment of the broad band at 852 cm^{-1} to the ν_3 $(UO_2)^{2+}$ is supported by its strong intensity. A weak band at 926 cm^{-1} (Musonoï) is more probably associated with the H_2O libration modes or the δ U-OH bending vibration than with the ν_3 $(UO_2)^{2+}$ vibration.

Chemical formula of pseudojohannite

The simplified chemical formula of pseudojohannite has been reported as $Cu_5(UO_2)_6(SO_4)_3(OH)_{16}\cdot 14H_2O$ in the original publications (Ondruš et al. 1997, 2003), based upon the chemical analysis reported in Table 4 and the unit-cell volume of 1081.2 $Å^3$. The number of O atoms in the unit cell can be estimated by comparison with the average volume of oxygen ions in some zippeite-group minerals and in johannite (Table 6). The number of anions is likely to be a multiple of 2 (no O atom on special position); also, the unit cell is likely to contain an integer number of U and S atoms. Following these considerations, we conclude that pseudojohannite contains 70 O atoms per unit cell, leading to the empirical formula $Cu_{6.52}U_{7.85}S_{4.02}O_{70}H_{55.74}$. Introducing a zippeite-type layer (Brugger et al. 2003; Burns et al. 2003), the simplified structural formula becomes $Cu_{6.5}[(UO_2)_4O_4(SO_4)_2]_2(OH)_5\cdot 25H_2O$.

The presence of H_2O and OH groups is confirmed by the thermo-gravimetric analysis (Fig. 4; Table 7). Pseudojohannite dehydrates and dehydroxylates in the range 55–625 °C in several steps. The mineral looses 9.10 wt% corresponding to ~$18H_2O$ between 20 and 210 °C, and 4.85 wt% corresponding to ~$10H_2O$ between 210 and 625 °C. A further 4.6 wt% weight loss occurring between 625 and 800 °C is attributed to SO_3 and, possibly O_2, released from the thermal decomposition of anhydrous uranyl sulfate and copper uranates, probably resulting from the dehydration reactions. The IR spectrum shows that pseudojohannite contains non-equivalent groups of H_2O molecules (see above).

Discussion

The zippeite group of minerals is named after the mineral zippeite, $K_3(H_2O)_3[(UO_2)_4(SO_4)_2O_3(OH)]$ (Burns et al. 2003; Frondel et al. 1976). The zippeite group is defined by a characteristic topology of the uranyl sulfate layers (Brugger et al. 2003; Burns et al. 2003). Both monovalent and bivalent cations can occur in the interlayer, and pseudojohannite belongs to the second category. Zippeite containing the divalent cations Mg, Co, Ni, and Zn have been reported and/or synthesized (Burns et al. 2003; Frondel et al. 1976). Frondel et al. (1976) attempted to synthesize Cu-bearing zippeites, but obtained only johannite or

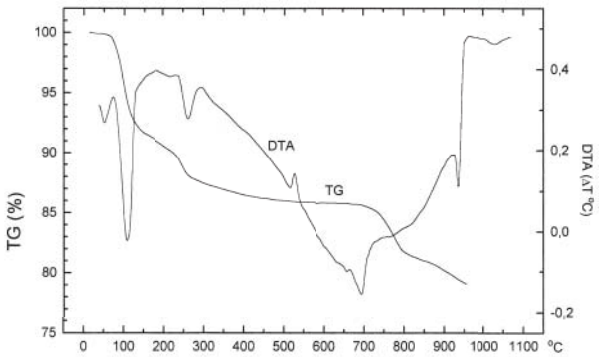

Figure 4. Thermogravimetric (TG) and differential thermogravimetric (DTG) curves of pseudojohannite from Jáchymov. TG-750 Stanton-Redcroft microthermobalance, sample weight 1.957 mg, 10 °C/min, dynamic air atmosphere, 10 mL/min.

Table 6. Comparison of the average volume occupied by anions in some zippeite-group minerals and in johannite

Mineral	Formula	Z	*V* (Å³)	Z*N_{anions}	V (Å³/Ox)	Ref
Marécottite	$Mg_3(H_2O)_{18}[(UO_2)_4O_3(OH)(SO_4)_2]_2(H_2O)_{10}$	1	1422.1(9)	68	20.91	1
Magnesium-zippeite	$Mg(H_2O)_{3.5}(UO_2)_2(SO_4)O_2$	8	2110.2(2)	108	19.54	2
SZIPPMg	$Mg_2(H_2O)_{11}[UO_2)_2(SO_4)O_2]_2$	4	2684.6(2)	124	21.65	2
Johannite	$Cu(UO_2)_2(SO_4)_2(OH)_2\cdot 8H_2O$	1	469.85	22	21.36	3
Pseudojohnannite	$Cu_{6.5}[(UO_2)_4O_4(SO_4)_2]_2(OH)_5\cdot 25H_2O$	1	1371.9(5)	70	19.46	

Note: References are (1) Brugger et al. (2003); (2) Burns et al. (2003); (3) Mereiter (1982).

basic copper sulfates together with sodium-zippeite or zippeite. The name "cuprozippeite" has been given by Boldyrev (1935) to a mineral containing 5 wt% CuO, but it is not known whether the material is related to the zippeite group (Frondel et al. 1976).

Until recently, the nature of the zippeite group was the subject of great confusion, especially regarding the divalent members of the group. Crystal structure refinements on natural (marécottite; Brugger et al. 2003) and synthetic zippeites (Burns et al. 2003) have revealed that the confusion is due to a great variability in the arrangement of the interlayer cations, resulting in different unit cells and cell volumes for zippeites containing divalent cations (Table 6).

Some level of disorder is common in the interlayers of zippeite-group minerals. The different configurations result in different distances between the zippeite-type layers (Fig. 5). In the crystal structure of magnesium-zippeite, two O atoms at opposite apices of each Mg-octahedron are shared with uranyl groups ($[UO_2]^{2+}$) from two adjacent zippeite-type layers (Fig. 5). This arrangement results in a relatively short distance between two uranyl-sulfate layers (d_z = 7.10 Å). In contrast, marécottite contains a hydrated layer of $Mg(H_2O)_6$ octahedra, and the zippeite-type layers are bound only by hydrogen bonding. This arrangement results in an increase in d_z to 9.47 Å. The synthetic phase SZIPPMg (Burns et al. 2003) has an intermediate configuration where Mg-octahedra share only one oxygen with a uranyl group (d_z = 9.03 Å). The size of the Mg- and Jahn-Teller distorted Cu-octahedrons are similar (Mg-O 1.9 to 2.5 Å in zippeites; Cu-O 1.9 to 2.4 Å in johannite). Hence, we can assume that the $Cu\Phi_6$ polyhedra (Φ = O,H_2O,OH) in pseudojohannite do not directly connect to two adjacent uranyl-sulfate layers, because of the long d_z of 9.16 Å. The metal:S ratio in pseudojohannite is higher than in other zippeite-group minerals, indicating that some, or all, of the $Cu\Phi_6$ polyhedrons are linked together.

The failure to locate the Cu atoms in pseudojohannite illustrates the fundamental difficulty of ab-initio structure solution from powder diffraction data, which originates from the 1-dimensional nature of the data, compared with 3-dimensional single-crystal data. This problem is particularly acute for minerals containing heavy atoms such as uranium, for which the X-ray diffraction patterns are dominated by scattering from the U atoms. The topology of the uranyl-sulfate layers plays a fundamental role not only for the classification of uranium minerals, but also in controlling their physical and chemical properties (Burns 1999). Hence, the ability of powder diffraction methods to reveal the topology of the uranyl framework opens new means to study the complex, and often fine grained uranyl minerals that are prevalent in areas where acid drainage waters interact with U-bearing ores or wastes (Finch and Murakami 1999).

TABLE 7. Thermogravimetric analysis of pseudojohannite from Jáchymov

Temperature range (°C)	Mass loss (mg)	Mass loss (wt%)	Attribution
55–210	0.178	9.10	18.34 H_2O
210–625	0.095	4.85	9.79 H_2O
55–625	0.273	13.95	28.13 H_2O
625–800	0.090	4.60	2.61 SO_3

Note: Decomposition process proceeds continuously at temperatures higher than 800 °C.

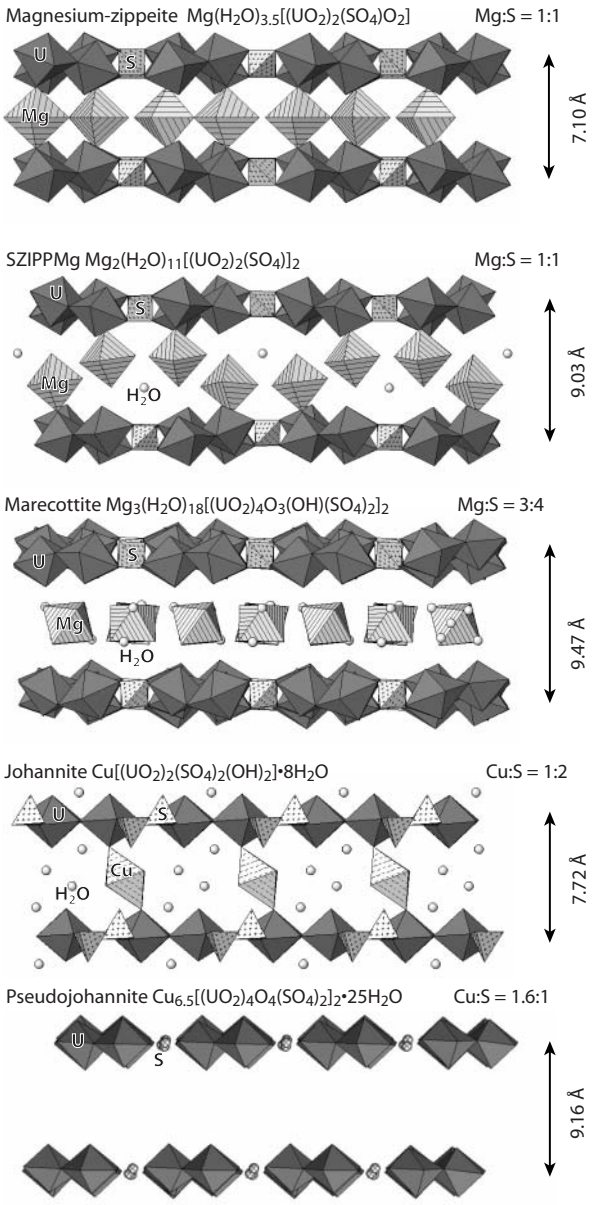

FIGURE 5. Comparison of the stacking and interlayer topology in the crystal structures of magnesium-zippeite (Spitsyn et al. 1982; Brugger et al. 2003), SZIPPMg (Burns et al. 2003), marécottite (Brugger et al. 2003), and johannite (Mereiter 1982) with pseudojohannite.

ACKNOWLEDGMENTS

We are grateful to Sergey Krivovichev and an anonymous reviewer for helpful comments. This work was partly funded by an Australian Research Council QEII fellowship to J.B. The synchrotron work was performed at the Australian National Beamline Facility with support from the Australian Synchrotron Research Program, which is funded by the Commonwealth of Australia under the Major National Research Facilities Program.

REFERENCES CITED

Altomare, A., Cascarano, G., Giacovazzo, G., Guagliardi, A., Burla, M.C., Polidori, G., and Camalli, M. (1994) SIRPOW.92-a program for automatic solution of crystal structures by direct methods. Journal of Applied Crystallography, 27, 435–436.

Barlett, J.R. and Cooney, R.P. (1989) On the determination of uranium-oxygen bond

lengths in dioxouranium(VI) compounds by Raman spectroscopy. Journal of Molecular Structure, 193, 295–300.

Boldyrev, A.K. (1935) Treatise on Descriptive Mineralogy. Leningrad, part 3 (cited from Frondel et al. 1976; in Russian).

Brugger, J., Burns, P., and Meisser, N. (2003) Contribution to the mineralogy of acid drainage of uranium minerals: marécottite and the zippeite group. American Mineralogist, 88, 676–685.

Burns, P., Deely, K., and Hayden, L. (2003) The crystal chemistry of the zippeite group. Canadian Mineralogist, 41, 687–706.

Burns, P.C. (1999) The crystal chemistry of uranium. In P.C. Burns and R. Finch, Eds. Uranium: mineralogy, geochemistry and the environment, 38, p. 23–90. Reviews in Mineralogy, Mineralogical Society of America, Chantilly, Virginia.

Čejka, J. (1999) Infrared spectroscopy and thermal analysis of uranyl minerals. In P.C. Burns and R. Finch, Eds., Uranium: mineralogy, geochemistry and the environment, 38, p. 521–622. Reviews in Mineralogy, Mineralogical Society of America, Chantilly, Virginia.

Čejka, J., Urbanec, Z., Čejka, J., Jr., and Mrázek, Z. (1988) Contribution to the thermal analysis and crystal chemistry of johannite $Cu[(UO_2)_2(SO_4)_2(OH)_2].8H_2O$. Neues Jahrbuch für Mineralogie, Abhandlungen, 159, 297–309.

Čejka, J., Sejkora, J., Mrázek, Z., Urbanec, Z., and Jarchovsky, T. (1996) Jáchymovite, $(UO_2)_8(SO_4)(OH)_{14}{\cdot}13H_2O$, a new uranyl mineral from Jáchymov, the Krusné Hory Mts., Czech Republic, and its comparison with uranopilite. Neues Jahrbuch für Mineralogie, Abhandlungen, 170, 155–170.

Finch, R. and Murakami, T. (1999) Systematics and paragenesis of uranium minerals. In P.C. Burns and R. Finch, Eds., Uranium: mineralogy, geochemistry and the environment, 38, p. 91–179. Reviews in Mineralogy, Mineralogical Society of America, Chantilly, Virginia.

Frondel, C., Ito, J., Honea, R.M., and Weeks, A.M. (1976) Mineralogy of the zippeite-group. Canadian Mineralogist, 14, 429–436.

Garrett, R.F., Cookson, D.J., Foran, G.J., Sabine, T.M., Kennedy, B.J., and Wilkins, S.W. (1995) Powder diffraction using imaging plates at the Australian National Beamline Facility at the Photon Factory. Review of Scientific Instruments, 66, 1351–1353.

Glebov, V.A. (1989) Stretching vibrations frequencies and interatomic distances in uranyl compounds. In B.N. Laskorin and B.F. Myasoedov, Eds., Uranium chemistry, p. 68–75. Nauka, Moscow (in Russian).

Hester, J., Garrett, R.F., Cookson, D.J., and Hunter, B. (1999) Phython PDA. Australian National Beamline Facility local web page, http://www.ansto.gov.au/natfac/ANBF/ppda/ppdapage.html.

Holland, T.J.B. and Redfern, S.A.T. (1997) Unit cell refinement from powder diffraction data: the use of regression diagnostics. Mineralogical Magazine, 61, 65–77.

Hunter, B.A. (1998) Rietica-A Visual Rietveld Program. Commission for Powder Diffraction Newsletter, 20, 21.

Le Page, Y. and Flack, H.D. (1995) CREDUC Xtal 3.5 User's Manual, edited by S.R. Hall, G.S.D. King, and J.M. Stewart. University of Western Australia, Lamb, Perth.

Libowitzky, E. (1999) Correlation of O-H stretching frequencies and O-H…O hydrogen bond lengths in minerals. Monatshefte für Chemie, 130, 1047–1059.

Meisser, N. (2003) Uranium mineralogy in the Aiguilles Rouges Massif (Western Alps). Science Faculty, University of Lausanne, Switzerland. 251 pp. (in French).

Meisser, N., Brugger, J., and Lahaye, Y. (2002) Mineralogy and acid-mine drainage of La Creusaz uranium prospect, Switzerland. In B. Kríbek and J. Zeeman, Eds., Uranium Deposits, p. 147–150. Czech Geological Survey, Prague.

Mereiter, K. (1982) Die Kristallstruktur des Johannites, $Cu(UO_2)_2(OH)_2(SO_4)_2{\cdot}8H_2O$. Tschermaks Mineralogische und Petrographische Mitteilungen, 30, 47–57.

Ondruš, P., Veselovský, F., Skála, R., Císařová, I., Hloušek, J., Frýda, J., Vavřín, I., Čejka, J., and Gabašová, A. (1997) New naturally occurring phases of secondary origin from Jáchymov (Joachimsthal). Journal of the Czech Geological Society, 42, 77–107.

Ondruš, P., Veselovský, F., Gabašová, A., Hloušek, J., and Šrein, V. (2003) Supplement to secondary and rock-forming minerals of the Jáchymov ore district. Journal of the Czech Geological Society, 48, 149–155.

Sejkora, J., Čejka, J., and Ondruš, P. (2000) New data of rabejacite (Jáchymov, the Krusné Hory Mts., Czech Republic). Neues Jahrbuch für Mineralogie Monatshefte, 7, 289–301.

Spitsyn, V., Kovba, L., Tabachenko, V., Tabachenko, N., and Mikhaylov, Y. (1982) To the investigation of basic uranyl salts and polyuranates. Izv. Akad. Nauk SSSR, Ser Kim, 1982, 807–812 (in Russian).

Visser, J.W. (1969) Fully automatic program for finding the unit cell from powder data. Journal of Applied Crystallography, 2, 89–95.

MANUSCRIPT RECEIVED DECEMBER 24, 2004
MANUSCRIPT ACCEPTED DECEMBER 29, 2005
MANUSCRIPT HANDLED BY PETER BURNS